24th COBEM - 2017

24th ABCM International Congress of Mechanical Engineering
December 3-8, 2017, Curitiba, PR, Brazil

COBEM-2017-0628
MODELLING A SUBSEA HYDRAULIC ACTUATOR FOR ULTRA-DEEP WATER

R. Goularte
V. De Negri
Federal University of Santa Catarina, Department of Mechanical Engineering, Florianópolis, Brazil
rafael@laship.ufsc.br , victor.de.negri@ufsc.br

A. Orth
Bosch Rexroth AG, Lohr am Main, Germany
alexandre.orth@boschrexroth.de

Abstract. *The objective of this work is to analyze the dynamic performance of a Subsea Hydraulic Actuator connected to a Hydraulic Power Unit (HPU) which constitutes a Hydraulic Positioning System using Speed Controlled Pump. This system is designed to operate on a Wet Christmas Tree (WCT) installed in a depth of 3.300 meters. A detailed mathematical model was developed representing the system dynamic and static behavior. In this way, the results obtained through simulation are presented, demonstrating the critical points and advantages of using the selected layout. The evaluated parameters are the pressures in the hydraulic cylinder chambers, valve operating time response, positioning capacity of the actuation system, the friction forces acting on the gate valve and the system energy consumption.*

Keywords: *Marine and Offshore Systems, Ultra-deep Water, Hydraulic Actuators, Subsea Oil & Gas.*

1. INTRODUCTION

Brazilian's oil and gas exploration industry has grown fast in recent years with the discovery of new reserves in the pre-salt layer. The investment made by this industry produces a demand for equipment for oil exploration. A great challenge for pre-salt exploration is the environment where the equipment will be used. The pre-salt reserves are in regions of maritime ultra-deep water, where the depth corresponds to the range from 1.830 to 3,000 meters. The design of equipment to operate in these conditions should take into consideration factors such as external high pressure and the difficult access to perform maintenance. Given these circumstances, the equipment must operate with minimal corrective action for at least 25 years.

One key equipment for oil production is the Wet Christmas Tree (WCT), which is connected to the subsea production wellhead. The purpose of the WCT is to control the flow of fluid extracted or injected into the reservoir and thus ensures proper oil drilling activity. It is noteworthy that WCT also contributes to the sealing of the wellhead in situations of emergency (leakages or obstruction in the pipeline, electric signal interruption and human error) while driving oil to the Floating Production Storage and Offloading (FPSO). The flow control of each fluid leaving or entering the reserve is conducted with the use of an actuator valve. According to Cezar *et al* (2015) each WCT that will be to applied in the pre-salt operations has approximately 20 actuators installed, thus guaranteeing a safe operation of the oil exploration system (Gerngross, 2014; Bai, 2010).

2. SUBSEA ACTUATOR VALVE AND POWER UNIT

The valve actuator structure is composed by three basic elements: valve, bonnet and actuator. The types of such elements are diverse and their choice will depend on their application in the exploration operation. The actuators can be of the electrical or hydraulic types and the valves can be accent choke valve, check valve, gate valve or ball valve. So the bonnet is only a coupling element that makes the connection between the actuator and valve selected. In Figure 1 it is shown a design of a Subsea Valve Actuator (SVA) assembly which uses a hydraulic actuator operating a gate valve, such design which will be approached in this work.

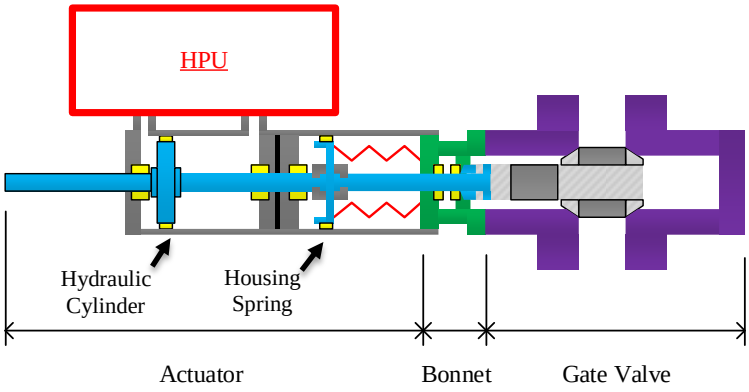

Figure 1 – Example a Subsea Valve Actuator (SVA).

The gate valve performs an important function regarding to the system safety including, for example, the injection of chemicals until closing of the well. Therefore, the valve stays closed for short periods. The interruption of power supplied to the actuators results in the immediate shutdown of production by closing the gate valve. The use of this valve design is due to the fact that it has a minimal obstruction to the passage of fluids when fully opened which results in low pressure drop. This is because the shutter acts perpendicular to the fluid flow line. The gate valve is not recommended for flow control because the intermediate positions promote an abrupt change in fluid velocity through the valve and the sealing surfaces may suffer erosion wear (Mashiba, 2011).

The hydraulic actuators have the advantages of great reliability, low complexity and the fact that they do not require power to maintain a specific position once the actuator ports are closed. Additionally, considering the spring installed in the SVA, no external energy is required to return the actuator in emergency situations. Therefore, the opening and closing of the valve is carried out by the action of an electro-hydraulic actuator. In Figure 2 an example of hydraulic circuit of the Hydraulic Positioning System using Speed Controlled Pump (HPS-SCP) is shown.

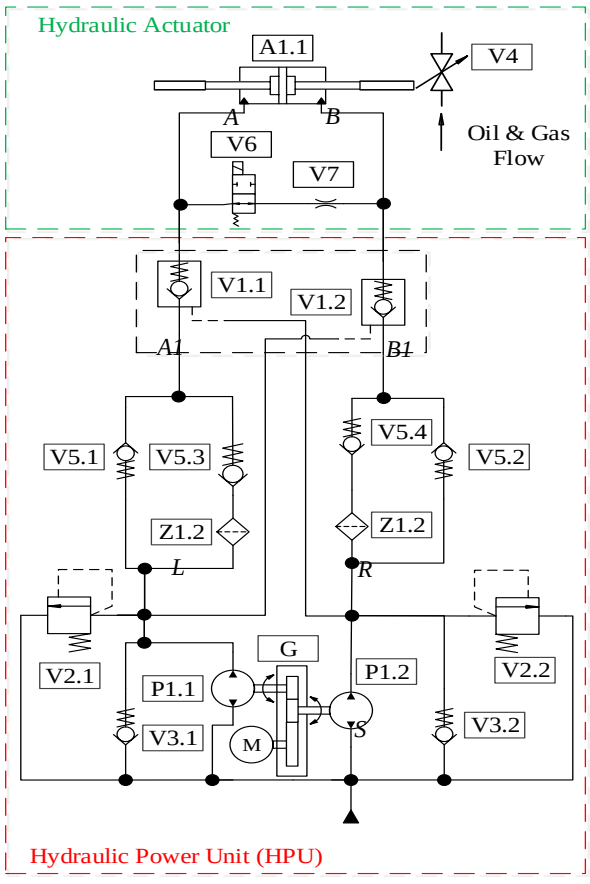

Figure 2 – Diagram of the Hydraulic Positioning System using Speed Controlled Pump (HPS-SCP).

The hydraulic system is composed of two piloted check valves (V1.1 and V1.2), two relief valves (V2.1 and V2.2) for safety, six check valves (V3.1, V3.2, V5.1, V5.2, V5.3 and V5.4), two oil filters (Z1.1 and Z1.2), one 2/2 normally open directional on/off valve (V6), one flow control valve (V7), two pump-motors (P1.1 and P1.2), a cylinder (A1.1), a gearbox (G) and a servomotor (M). The control of the actuator position is not by a directional valve but by the variation of the angular velocity of the electric servomotor.

The HPS-SCP follows the hydraulic zone concept that is applied in aviation industry. The concept proposes to embed the HPU into the actuator. Additionally, this technology eliminates umbilical hydraulic lines and, consequently, friction losses, and reduces weight and space occupied in topside. This system design has the necessary characteristics to attend the demand of the oil and gas exploration industry reducing the operational costs in ultra-deep-waters.

3. MATHEMATICAL AND COMPUTATIONAL PROCEDURE

The evaluation of the system performance is based on the analysis of the opening and closing conditions of the gate valve. In this study, a mathematical model was developed and the system performance evaluated using co-simulation. The component models were based on the equations of conservation of energy, mass, and quantity of movement. The model of the hydraulic system and the controller are implemented on the simulation software Simster. The forces acting in the gate valve, the effect of the pressure caused by the water column and the pressure drop along the oil pipe are modeled in MATLAB Simulink™. The two simulations run simultaneously in such away the system behavior can be analyzed. The forces acting in the electro-hydraulic actuator system are indicated in Figure 3, where:

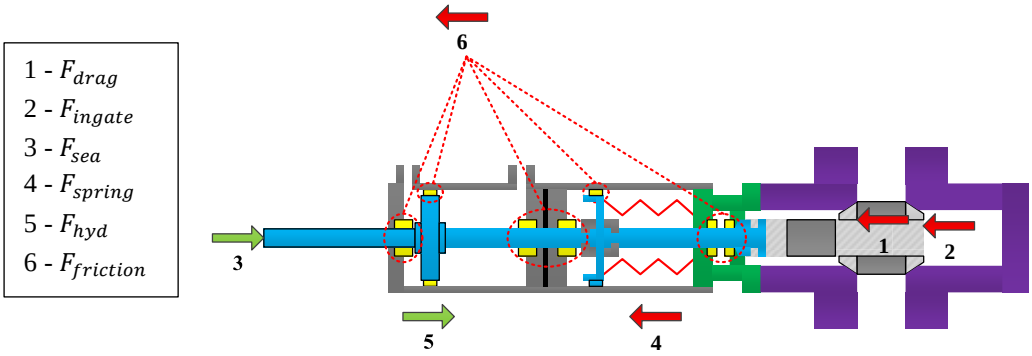

Figure 3 – The forces acting the opening the gate valve.

The meaning of each of the forces will be explained in the next sections and their mathematical definition will be presented.

3.1 Gate Valve

The subsea actuator is installed in the seabed in the WCT and it works as control device between the oil well and the FPSO. Thus the length of the oil pipeline is divided into two parts LDA and AG as it is shown in Figure 4.

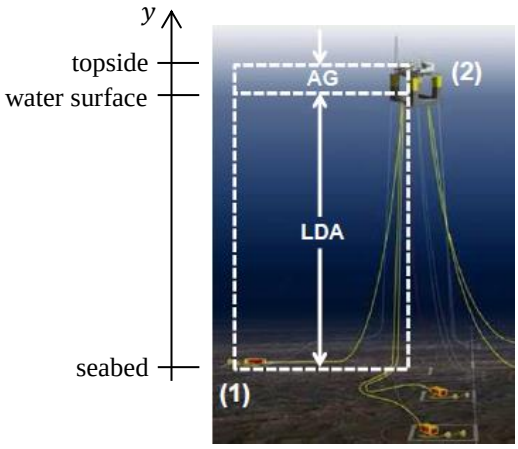

Figure 4 - Representation of the water column above the actuator adapted from Mashiba (2011).

The LDA value represents the distance between the water surface and the point where the WCT is installed. The AG value represents the distance between the water surface and the oil separation/reservoir in the FPSO for oil storage. The pressures (p_1 and p_2) at the points (1) and (2) are, respectively, the internal pressure in the oil well (p_{well} = 690 MPa) and the pressure in the separator in the platform (p_{sep} = 30 MPa). The flow of oil along the pipeline can be represented with the Bernoulli's equation:

$$\frac{p_1}{\gamma} + \frac{v_1^2}{2 \cdot g} + z_1 = \frac{p_2}{\gamma} + \frac{v_2^2}{2 \cdot g} + z_2 + h_{valve} + h_{line} \tag{1}$$

where h_{valve} is the minor loss in the gate valve, h_{line} is the loss due to the friction of the production fluid with the inner surface of the pipeline, g is gravitational acceleration, v_1 is the velocity of the fluid inside the oil reservoir ($v_1 \cong 0$) , v_2 is the velocity of the fluid at the inlet of the oil separator, γ is the specific weight of the production fluid, z_1 is the position of the hydraulic actuator ($z_1 = 0$) and z_2 is the position of the oil separator.

Manipulating Eq. 1 gives the equation of average velocity of the oil flow along the pipeline. In the analysis of this study the pipeline length (L) was considered 13 km. ρ_{FP} is the specific mass of the production fluid. However, to determine the average velocity, it is necessary to know the pressure loss coefficient at the valve (K) and the pipeline friction factor (f). Both variables are dependent on the position of the gate valve.

$$v(x) = \sqrt{\frac{2[(p_1 - p_2) - \rho_{FP} \cdot g \cdot (LDA + AG)]}{\rho_{oil} \cdot \left(1 + K(x) + f(x) \cdot \frac{L}{D}\right)}} \tag{2}$$

The friction factor is determined by the solution of Eq. 3, it is known as implicit Colebrook-White equation.

$$\frac{1}{\sqrt{f(x)}} = -2 \cdot \log\left(\frac{\varepsilon}{3.7 \cdot D} + \frac{2.51 \cdot \nu}{v(x) \cdot D \cdot \sqrt{f(x)}} \right) \tag{3}$$

where D is the pipeline diameter, ν is the kinematic viscosity of the production fluid and ε is the average roughness of the inner wall of the pipeline.

The determination of the valve pressure drop is proportional to the position opening of the gate valve. Fig. 5 shows all stages of the gate valve opening.

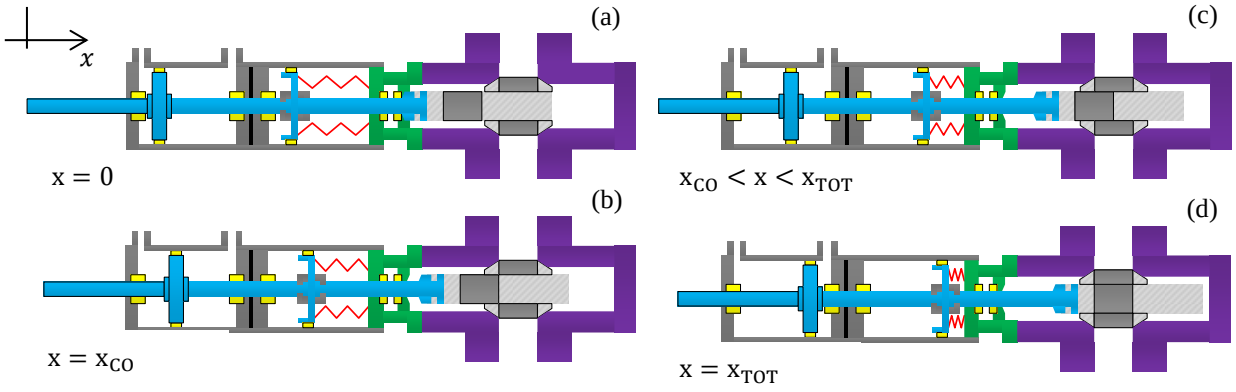

Figure 5 - Representation of the stages an gate valve (a) closed, (b) crack-open, (c) semi-open and (d) completely open.

When the shutter is in the position $x = 0$, the valve is fully closed and flow rate is zero. $x = x_{CO}$ is the crack-open moment that initiates the passage of fluid through the valve and $x = x_{TOT}$ represents the valve fully opening and the losses are minimal. According to Mashiba (2011), the valve load loss coefficient depends on the percentage of opening of the gate valve, that is:.

$$K(x) = 1984.\, e^{-0.735.h(x)^{0.545}} + 0.1 \tag{4}$$

where the variation of the minor loss is proportional to the percentage of opening:

$$h(x) = \begin{cases} 0 & if\ 0 < x \leq x_{co} \\ \dfrac{x - x_{co}}{x_{tot} - x_{co}}.100 & if\ x_{co} < x \leq x_{tot} \end{cases} \quad (5)$$

Therefore, the downstream pressure at the gate valve can be determined by

$$p_j(x) = \begin{cases} p_{sep} + \rho_{oil} \cdot g \cdot (LDA + AG) & if\ 0 \leq x < x_{co} \\ p_m - K(x) \cdot \rho_{oil} \cdot \dfrac{v^2(x)}{2} & if\ x_{co} \leq x < x_{tot} \end{cases} \quad (6)$$

where p_{sep} is the pressure on the surface separator install in the topside. Knowing the gate valve upstream and downstream pressures, it is possible to determine the pressure differential and the drag frictional force (F_{drag}). As illustrate in the Fig. 3 the friction force is due to the contact between the seals with the seat of gate valve. This force is the main component of the total friction force.

$$F_{drag}(x) = A_{GateValve}(x) \cdot \left(p_{well} - p_j(x)\right) \quad (7)$$

where $A_{GateValve}$ is it is the difference between maximum area with the oil pass-through of the gate valve.

The valve body cavity always has internal pressure equal to the upstream pressure as illustrate in the Fig. 3. The pressure acting on the area of rod cross section is the pressure in the oil reservoir, i.e. the pressure upstream of the valve, resulting on a force expressed by

$$F_{ingate} = \frac{\pi}{4} \cdot D_{HP}^2 \cdot p_{well} \quad (8)$$

The actuator is subjected to the environment pressure, i.e. the external pressure to the actuator is equivalent to the pressure coming from the water sea column above it. The actuator used a symmetric cylinder as shown in Fig. 3; the actuator rod is exposed to the marine environment. Therefore, there is external force acting on the actuator, which is defined by Equation 9.

$$F_{sea} = \frac{\pi}{4}.D_{rod}^2.\rho_{sea}.g.LDA \quad (9)$$

where D_{rod} is the diameter of the actuator rod and ρ_{sea} is the density of sea water.

3.2 Electro-Hydraulic Actuator

A typical spring used in ultra-deep waters is a Belleville spring. It has the ability to tolerate high compression loads and has a compact geometry. However, it presents a nonlinear load behavior when force is correlated to deformation. The force of deformation is presented in Eq.10 where, k_1 and k_2 are spring constants and L_1 is the initial preload spring compression. The preload will ensure the positioning of the closed valve when it is fully closed during a normal or emergency operation situation.

$$F_{spring}(x) = k_1.(L_1 - x(t))^2 + k_2.(L_1 - x(t)) \quad (10)$$

The hydraulic force is defined by the pressure differential between the pressures p_a and p_b in the cylinder chambers, resulting on

$$F_{hydraulic}(t) = A_{cylinder}(t) \cdot [\, p_a(t) - p_b(t)\,] \quad (11)$$

The friction force ($F_{friction}$) includes the friction at the actuator and bonnet. Thus the parameters were inserted in the mathematical model of hydraulic cylinder friction.

3.3 DC Motor

According to Chen *et al* (2011) the Brushless DC Motor (BLDC) present lower cost and mid-size. It fits perfectly when the implementation is on a Subsea Actuator Valve with compact dimensions and at an reasonable cost. Furthermore, the rotational frequency control can be easily implemented in a brushless motor. With the electric voltage

supplied, it is possible to control the speed of operation in a simple way. Eq. 12 represents the voltage balance equation for the DC motor.

$$V_{in}(t) = K_e \cdot \dot{\theta}(t) + R \cdot i_a(t) + L \cdot \frac{di_a}{dt} \tag{12}$$

where, R and L are the resistance and inductance of the windings respectively, V_{in} is voltage, i_a current, $\dot{\theta}$ is the electrical angular velocity and K_e is the BEMF (Back Electromotive Force) constant.

The mechanical movement equation is represented by

$$T_{mec}(t) = T_{eletric}(t) - B \cdot \dot{\theta}(t) - T_{load}(t) \tag{13}$$

where $T_{mec}(t)$ is the mechanical torque, $T_{eletric}$ is the torque electric, B is a viscous friction and T_{load} is torque load.

One of the focuses of this paper is the analysis power consumed by the system. The consumed electric power can be defined by Eq. 14

$$P_{eletric}(t) = V_{in}(t) \cdot i_a(t) \tag{14}$$

where $P_{eletric}$ electric power that is supplied to the DC motor, V_{in} the voltage defined by the control for the rotation control of the electric motor and i the electric current in the electric motor.

4. RESULTS AND DISCUSSION

A trapezoidal signal was used as a reference for opening and closing the gate valve. This type of signal was choose to be avoiding the peaks of electric current and, consequently, reducing the power consumed by the electric motor. Furthermore, this type of signal avoids the propagation of shockwaves as when it has a rapid opening or closing of the gate valve. It can promote the release/containment of a significant amount of energy from the oil well to the pipeline.

The reference signal and the ability of the proposed system on controlling the actuator position directly by speed control of pumps are analyzed in the Fig. 6a). It shows the overlapped between the position of the hydraulic cylinder and the reference signal.

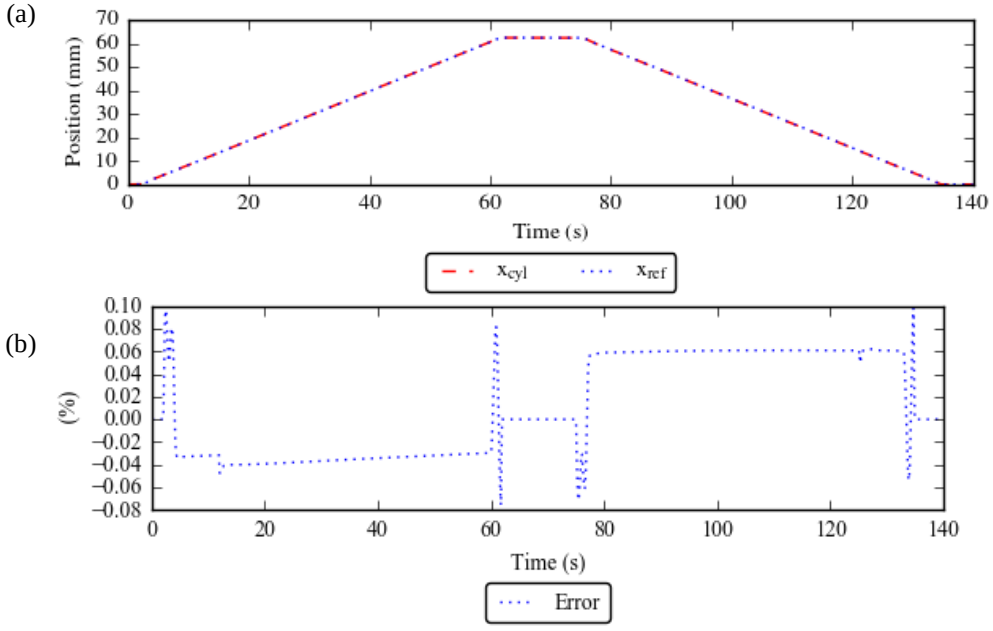

Figure 6 – Positon and error for electro-hydraulic actuator.

The maximum positioning error identified during the opening and closing process of the gate valve was 0.1% for the operating condition of 3,330 meters depth than it is showing in Fig.6b). The low error values obtained are directly related to the use of the brushless DC motor because it has a fast dynamic response, allowing the correction of the trajectory even with the oscillations of load during the opening and closing of the gate valve. The maximum time set for each operation, opening and closing, was 60 seconds. The power consumptions for depths of 2,600 and 3,300 meters are showing in the Fig. 8.

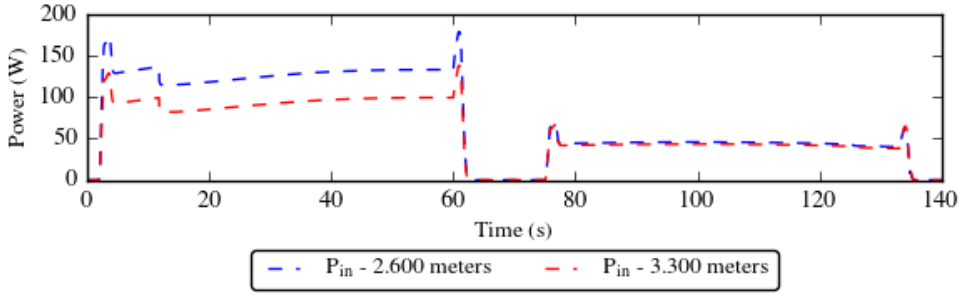

Figure 7 – Power consumed for depths of 2.600 and 3.300 meters..

The increase in consumption at lower depth was approximately 30% since the force exerted by the water column helps the opening movement of the actuator according to Eq.9.. However, in the return of the actuator the energy consumption remained similar for both situations since the force provided by the mechanical spring assists the return movement. Pumps P1.1 and P1.2 perform the control of the speed with which the hydraulic cylinder returns. The power values found refers only to the actuator movement and do not represent the total system consumption that would include the energy supply to temperature, pressure, contaminant, position and frequency sensors. The power consumption is lower than 200 W, which it is the maximum limit needed from the Subsea Module Control (SCM).

An evaluation based only on the power consumed by the actuation system is not totally representative. So it is necessary to determine the energy consumed during an operating cycle. The following equations are used to calculate the energy consumption in the system:

$$E_c(t) = \int q_c(t) \cdot \Delta p_c(t) \cdot dt \tag{15}$$

$$E_l(t) = \int f_c \cdot \Delta p_c^2(t) \cdot dt \tag{16}$$

$$E_{in}(t) = \int V_{in}(t) \cdot i_a(t) \cdot dt \tag{17}$$

$$E_g(t) = \int T_g(t) \cdot \omega_g(t) \cdot dt \tag{18}$$

where E_c is the energy dissipated in the component, q_c is the flow rate through the hydraulic component, Δp_c is the pressure differential in the hydraulic components, E_l is the energy dissipated as internal leakage, E_{in} is the electric energy at system, E_g is the dissipated energy in the transmission box, T_g is the mechanical torque and ω_g the axis rotation. In Figure 9, the energy distributions are determined for an SVA during an operating cycle, allowing to understand the main sources of system energy losses. It consists of the complete opening and closing movement of the gate valve at a depth of 3,330 meters.

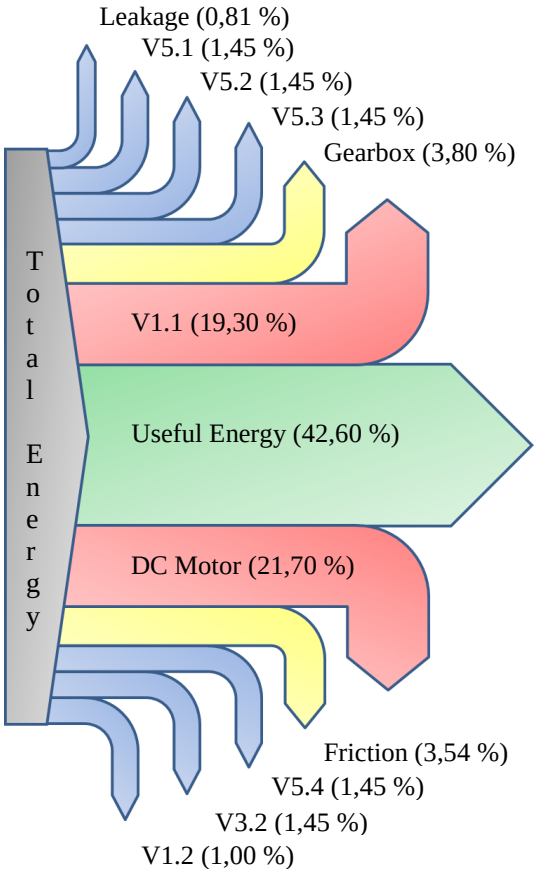

Figure 8 – Diagram showing the distribution of energy in SAV.

The main source of energy loss is at the electrical machine with 21.7%. The frequency converter loss is not included in this study. According to Minav (2015), the DC motor has two types of losses. Electrical machine losses are composed of the stator and rotor resistive losses, iron losses and additional losses. Mechanical losses include friction in the motor bearings what is dependent on the shaft speed, bearing type, properties of the lubricants and the load.

The second largest source of energy loss is valve V1.1 and it is represented in the Fig. 10 with the gauge pressures at three points (L, R and A1) in the hydraulic circuit.

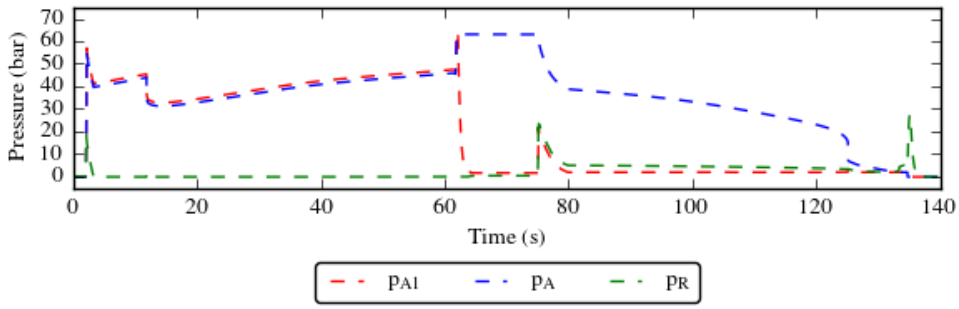

Figure 9 – Gauge pressure at points A, A1 and R.

During the opening of gate valve, in the range of 2 to 62 seconds, there is a small pressure differential between the points upstream (A_1) and downstream(A). The small pressure difference comes from the check valve (V3.1) with a pre-charge pressure (p_0). However, there is a discrepancy of the pressures in the range of 75 to 130 seconds. It indicates that valve V1.1 restricts the passage of hydraulic fluid. This behavior modifies the mechanism for controlling the actuator return speed. The control should be done by pump P1.1 but it is carried out by V1.1. The check valve throttle the hydraulic fluid passage and the energy present in the hydraulic fluid is dissipated as heat. The effect of the restriction is

a consequence of the low pilot pressure which it is insufficient for the unlocking of the valve V1.1. The procedure for opening by pilot is presented in Eq. 19 which defines percentage to open of the piloted check valve.

$$u = \begin{cases} 0 & if\ (p_R - p_{A1}) \leq 0 \\ \left(\dfrac{p_{A1} - p_A - p_0 + (p_R - p_{A1}) \cdot R}{dp}\right) & if\ (p_R - p_{A1}) > 0 \end{cases} \quad (19)$$

where R is the pilot area ratio, p_0 is the preload and dp the spring constant of the check valve.

The valve opening occurs when $(p_R - p_{A1}) > 0$. However, the differential pressure at point A and A1 are high as shown in Fig. 10. This behavior demands a higher pressure in the pilot which it is not achieved. The hydraulic force is not effective because the spring force assisted for the return movement. Consequently, there is a low pressure at the point B and R. The problem could be solved with increasing the value of the relation of areas of the pilot but the valves selected have the bigger ratio of areas of pilot offered in the catalog of the manufacturer.

5. CONCLUSIONS

The layout of a HPS-SCP has dynamic and static behavior in the observed conditions. The position control capability is dependent on the fast dynamics of the pump drive system; this is achieved due the characteristics of the DC Brushless Motor. The paper demonstrates that the simulation is a useful tool to evaluate and to consolidate the development of new mechanical systems and maybe the model can help to reduce the final costs of project. For a second phase of this project, experimental tests should be carried out for improving and validating the developed mathematical model. The model will be used to determine energy consumption at other elements present in the SAV such as sensors and frequency inverter.

6. ACKNOWLEDGEMENTS

The research was enabled by the financial support of CNPq and technical support of Bosch Rexroth AG.

7. REFERENCES

Gerngross, R and Orth, A., 2014. “Design of safe and reliable hydraulic systems for subsea applications”. 10 Nov 2015 <https://dc-us.resource.bosch.com/media/us/trends_and_topics_2/technical_papers/marine_offshore/deepseahydraulics.pdf>.

Bai, Y. and Bai, Q., 2010. *Subsea Engineering Handbook*. Elsevier, Houston, 1st edition.

Cezar, A. *et al*, 2015. “Subsea solution in the Pre-salt development projects”. In *Proceeding of the Offshore Technology Conference – OTC2015*. Houston.

Mashiba, M.H.D., *The influence of the operating and design parameters in the hydraulic actuation performance of subsea gate valves*. Master thesis, Federal University of Rio de Janeiro, Rio de Janeiro, Brazil.

Chen, C.H.; Chi, W.C.; Cheng, M.Y., “Regenerative braking control for light electric vehicles”. In *Proceeding of the 9th International Conference Power Electronics and Drive Systems*. Singapore.

Minav, T.A.; Heikkinen, J.E., Pietola, M. “Chapter 6 - Electric-driven Zonal Hydraulics in Non-Road Mobile Machinery”. In *New Applications of Electric Drives*, Dr. Miroslav Chomat, InTech, 2015. DOI: 10.5772/61793

8. RESPONSIBILITY NOTICE

The author(s) is (are) the only responsible for the printed material included in this paper.